High Intensity Above-Threshold Ionization of He

U. Mohideen*
Department of Physics, Columbia University, New York, New York 10027

M. H. Sher, H. W. K. Tom, G. D. Aumiller, O. R. Wood II, R. R. Freeman, and J. Bokor
AT&T Bell Laboratories, Holmdel, New Jersey 07733

P. H. Bucksbaum
Physics Department, University of Michigan, Ann Arbor, Michigan 48109-1120
(Received 16 November 1992)

This is the first high resolution measurement of the electron energy spectrum from high intensity above-threshold ionization (ponderomotive energy $\gg$ ionization potential $\gg h\nu$) at intensities up to 7×10^{15} W/cm^2. In contrast to previous work, we have used a short pulse and a large focal spot along with low gas densities to minimize the effect of ponderomotive forces and collisions. Existing models do not agree well with electron energy spectra for either linearly or circularly polarized light. The electron temperature is too hot for the implementation of 820 nm multiphoton ionized recombination type XUV laser schemes.

PACS numbers: 32.80.Rm

We report the first high resolution measurement of the electron energy distribution from high intensity above-threshold ionization (ATI) at intensities up to 7×10^{15} W/cm^2 with a short pulse. In the short pulse regime [1-4] the pulse is over before the electrons have been disturbed by the ponderomotive force: The electrons are therefore characteristic of the ionization intensity and not of the excitation geometry. Previous measurements of electron spectra in the so-called "long pulse regime" were dominated by the ponderomotive acceleration of the electrons, which is their quiver response to the oscillating electromagnetic field in the intensity gradient at the laser focus [1-6]. The measurements reported here are at intensities 30 times more intense than those previously published and allow us to test models of ATI in the high intensity limit when ATI models should be most valid, viz., ponderomotive energy $\gg$ ionization potential $\gg h\nu$.

ATI electron energy spectra from both linearly and circularly polarized light were measured. While the threshold intensities for multiphoton ionization agree with models of ATI [7-9], the electron spectra from linear or circular polarization differ markedly from theory. *The predicted preponderance of slow electrons from linearly polarized ATI is not observed.* This result is particularly noteworthy in light of recently proposed x-ray laser schemes that use multiphoton ionization to produce high ion stages in a relatively cold electron distribution [10-12].

These measurements are valuable because the ATI electron energy distributions contain minimal ponderomotive force contributions, despite the fact that the ponderomotive energy is much higher than the ionization potential of the parent atom. To achieve this, we require both a short pulse and a large focus. Our laser source is a colliding-pulse mode-locked laser [13] centered at 820 nm, amplified in a Ti-sapphire chirped-pulse amplifier [14]. It is capable of delivering 50 mJ pulses of 180 fs duration at 5 Hz. Laser pulses are focused with a 1 m lens into a vacuum chamber to a Gaussian waist of $\omega_0=35$ μm. After the lens the laser beam propagates almost entirely in vacuum. The electron energy spectra are measured with a field-free time-of-flight (TOF) spectrometer with a detection cone angle of 2° (3.8×10^{-3} sr collection solid angle) at the focus. Electrons are accelerated at the end of the TOF in order to level the detection efficiency. The intensities at the focus are calibrated by measuring Xe ion spectra and comparing to critical intensities in Refs. [7,9].

This system is highly insensitive to ponderomotive acceleration. A 100 eV electron produced at the peak of a 7×10^{15} W/cm^2 pulse gains less than 3.5 eV in radially traversing the beam. Most electrons gain much less energy as they are created off the beam axis and at different times during the pulse. The spectrometer has a resolution of 0.05 eV at an energy of 3 eV.

The electrons in our spectrometer are almost entirely from ATI in He. At these high intensities the electron energy distribution resulting from the ATI of He atoms is a good test of models of ATI. The threshold intensity for ionization according to the barrier suppression model is given by [3,4]

$$I_{\rm th}=I_p^4 c/128\pi Z^2 e^6, \quad (1)$$

where I_p is the ionization potential, Z is the charge state of the resulting ion, c is the speed of light, and e is the charge of an electron, all in cgs units. The ionization potential of He is 24.6 eV, and the second ionization potential ($He^{1+}\rightarrow He^{2+}$) is 54.4 eV. Therefore, He^{1+} should be formed at around 1.46×10^{15} W/cm^2 ($U_p=91$ eV) and there should be negligible amounts of He^{2+} below an intensity of 9×10^{15} W/cm^2. We measure the threshold intensity for ionization of $He^{1+}\rightarrow He^{2+}$ to be $\sim10^{16}$

0031-9007/93/71(4)/509(4)$06.00

W/cm^2, consistent with Eq. (1) [7,9]. Therefore at these intensities only He^{1+} is saturated.

We also take steps to eliminate background contaminants and space charge effects, which might alter the electron spectrum. The He gas pressure is maintained at 2×10^{-8} torr (density of 7×10^{8} atoms/cm^3) on a base pressure of 4×10^{-10} torr. The electron spectrum of the background gas is less than 12% of the He signal and is measured and subtracted. Because of the low pressures used in the experiment an electron suffers fewer than 10^{-5} collisions at the focus during the 180 fs laser pulse [15]. Also, complete ionization of the focal volume results in a space charge effect of less than 0.07 eV for any detected electron. Thus the spectra are essentially free of collisional and space charge effects.

In Fig. 1 we show the ATI spectrum of He obtained at an intensity of 7×10^{15} W/cm^2 (Xe^{7+} ion stage observed in ion spectra). The light is linearly polarized with the polarization axis oriented along the TOF axis. If the electric field in a monochromatic linear polarized plane wave is given by $\mathbf{E}(\mathbf{x},t)=E_0\boldsymbol{\varepsilon}_x\cos(kx-\omega t)$ then the ponderomotive energy (average energy of sinusoidally oscillating free electron) is

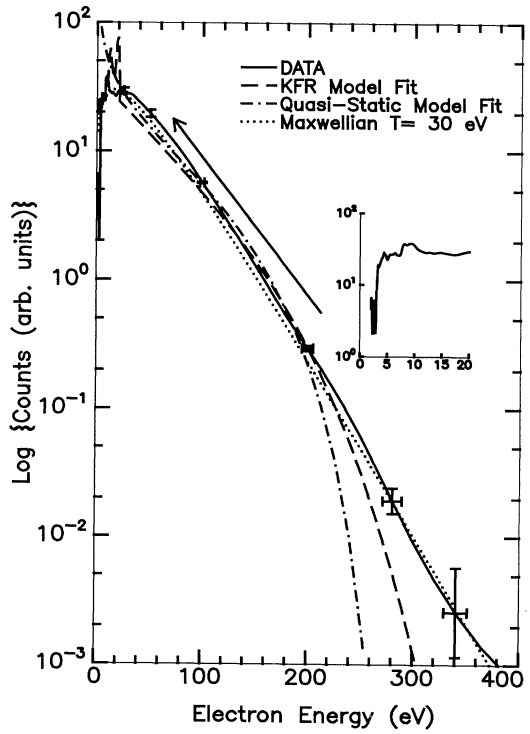

FIG. 1. The solid line is the electron energy spectrum obtained from the ATI of He with linearly polarized light at a peak intensity of 7×10^{15} W/cm^2. Error bars at representative points are shown. Vertical error bars are statistical. The horizontal error bars refer to the energy bin width. The KFR model fit and the quasistatic model fit to the data are shown. The Maxwellian fit is for an electron temperature (kT) of 30 eV.

$$U_p=e^2E_0^2/4m\omega^2, \tag{2}$$

where m is the mass of the electron and ω is the frequency of the light. At an intensity of 7×10^{15} W/cm^2 this ponderomotive energy is 430 eV. The He spectrum is due almost entirely to ATI from $He\rightarrow He^{1+}$ ($<5\%$ of He^{2+} measured). At these high intensities the electron energy distribution is continuous and does not show the Rydberg level structure that is seen in the ATI of rare gas atoms at lower intensities [1–4]. This is expected because at these intensities, the ponderomotive shift is many times the photon energy and therefore all multiphoton Rydberg level resonances are equally allowed. The overlap of so many Rydberg level resonances washes out any resonance structure. The fall from 20 to 400 eV for He is nearly exponential. An exponential-like decrease is generally predicted by Keldysh-Faisal-Reiss (KFR) theory [16–19] and the quasistatic theory of Corkum and Burnett [5,12].

The KFR theories [16–19] treat ATI as the transition of the bound electron state to a free electron state oscillating in the electromagnetic field of the laser (Volkov states). The transition probability for n-photon ionization per unit time per unit solid angle in linear polarization (polarization axis along the detector axis) is then

$$\frac{dW_n}{d\Omega}=\frac{1}{(2\pi)^2\hbar^4}(2m_e^3)^{1/2}(n\hbar\omega-U_p)^2 \times(n\hbar\omega-U_p-I_p)^{1/2}|\Phi(p)|^2J_n^2(\alpha,\beta), \tag{3}$$

where

$$J_n(\alpha,\beta)=\sum_{m=-\infty}^{m=\infty}J_{n-2m}(\alpha)J_m(\beta), \tag{4}$$

where J_n are the nth-order cylindrical Bessel functions and $\Phi(p)$ is the Fourier transformed wave function of He and p is the momentum of the outgoing electron, $p=(2m_e)^{1/2}(n\hbar\omega-U_p-I_p)^{1/2}$, and the arguments of the Bessel functions are $\alpha=2[U_p/m_e\hbar^2\omega^2]^{1/2}p$ and $\beta=-U_p/2\hbar\omega$. Only electrons along the polarization direction are detected in this experiment. According to this model it is the interference between the various dressed continuum states represented in Eq. (4) which give rise to the structure of the electron energy distribution. The rate of ionization is so nonlinear that it is reasonable to fit the electron energy distribution to one intensity. The best fit of the data by the KFR model occurs with a fit parameter $U_p=150$ eV. The fit is shown as a dashed line in Fig. 1. For this fit we used a $1s$ hydrogenlike wave function for He given by [20]

$$\Phi(r)=(1/\pi)^{1/2}(1.69/a_0)^{3/2}\exp(-1.69r/a_0). \tag{5}$$

The distribution is relatively insensitive to the exact nature of the wave function [18,19].

The model predicts more cold electrons and fewer hot electrons than shown in Fig. 1. Furthermore, the value of U_p required to fit the data suggests a much higher ionization intensity than expected. Earlier ionization yield

measurements have shown that the ionization threshold is very close to the value predicted by the barrier suppression model [7]. For He ionized with 820 nm light, this threshold intensity has $U_p = 91$ eV. Our fit value of $U_p = 150$ eV is significantly higher.

In the quasistatic model [5,12], electrons tunnel ionize with a probability that depends on the instantaneous laser electric field, and subsequently gain energy by classical acceleration in the laser field. Most of the electrons tunnel out near the crest of the electric field (where the electric field is a maximum) and then undergo equal and repeated amounts of acceleration and deceleration, thus leading to no net energy gain. Therefore, most of the electrons should have very little final kinetic energy. On the other hand, an electron released near a minimum (absolute value) in the electric field would pick up a kinetic energy corresponding to a quarter cycle of the electric field. This leads to a characteristic distribution given by Eq. (5) of Ref. [12]. The best fit of the quasistatic theory to the data is shown by the dash-dotted line in Fig. 1. We used a fit with the peak intensity corresponding to $U_p = 150$ eV (corresponding electric field) as before. Again, we used a single intensity to characterize the ionization because the ionization rate is so nonlinear. As with the KFR model, the tunneling model predicts more cold electrons and fewer hot electrons than are observed. This discrepancy is more severe for the electrons below 5 eV in the tunneling model because the electric field is treated classically and electrons are allowed to pick up energies below the photon energy.

The deficit of cold electrons and the excess of hot electrons would be much more extreme had we used a fit parameter of $U_p = 91$ eV as predicted by the ionization threshold measurements [7–9]. The excess of hot electrons observed may be explained by the survival of some of the atoms to higher intensities. A more complete fit taking into account the temporal shape of the laser pulse might predict such high intensity survival. However, the disagreement for cold electrons would be more extreme with temporal averaging. To eliminate the possibility that the experimental deficit of cold electrons was due to stray fields or ponderomotive deflection of electrons, we applied an extraction voltage to get the total yield, measured the angular distribution of electron emission by rotating the polarization axis with respect to the TOF detector, and then adjusted for the collection solid angle. In addition, we biased the front plate of the multichannel plate detector to ensure the quantum efficiency for all electrons was uniform.

In general, the electron spectra are hotter than predicted by the theories. One possible reason is the Coulomb effect of the residual ions, which have been ignored in the models. The long-range Coulomb force would allow the absorption of excess photons from the high intensity laser field by the quasifree electron, which could lead to a hotter electron distribution than predicted.

The electron energy distribution is important for implementation of proposed multiphoton-ionized recombination XUV laser schemes [5,10–12]. Here the atoms are multiphoton ionized in a high intensity laser to give rise to highly charged ion states surrounded by a cold electron distribution. Lasing occurs if the cold electrons recombine rapidly enough to invert the population of the lower lying excited states of the ions. The recombination rate necessary for inversion depends critically on the average kinetic energy of the electron distribution. The electron temperature should be less than one-tenth of the ionization energy of the atom or ion stage [10,11]. We can obtain the electron temperature by fitting the data to a Maxwellian energy distribution given by [21] $f(E) = 2(E/\pi k^3 T^3)^{1/2} \exp(-E/kT)$, where E is the energy of the electron and kT is the equivalent electron temperature. The dotted line in Fig. 1 shows the best Maxwellian fit to the data. The fit yields an electron temperature of 30 eV ($kT = 30$ eV). The electron temperature is thus on the order of the ionization energy of neutral He, which is 24.6 eV. The hot electron temperature observed would drastically reduce the recombination rate and make simple multiphoton-ionized recombination XUV lasers difficult to implement.

The electron spectrum obtained with circularly polarized light is markedly different from that obtained from linearly polarized light. Figure 2 is the electron energy distribution obtained with circularly polarized light produced with a zeroth-order quarter-wave plate at 815 nm. The peak intensity is 6×10^{15} W/cm^2, in an Airy focus with the first null at a radius of 52 μm. The light is better than 99.7% circularly polarized. The electron en-

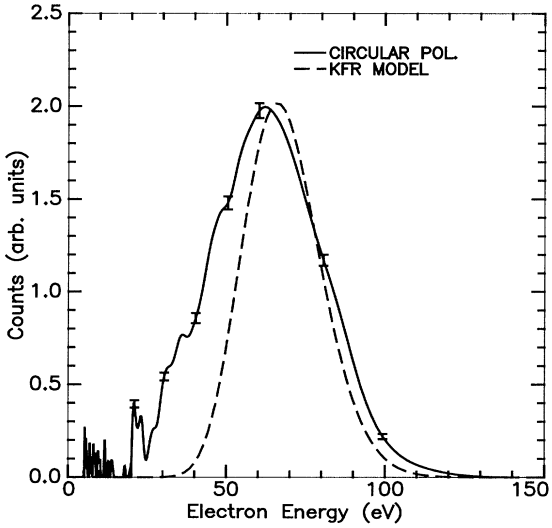

FIG. 2. The solid line is the electron energy spectrum obtained from the ATI of He with circularly polarized light at a peak intensity of 6×10^{15} W/cm^2. Error bars at representative points are shown. Vertical errors bars are statistical. The energy bin width is less than 1.0 at 100 eV and decreases roughly as (energy)$^{-3/2}$. The KFR model fit is for an intensity corresponding to $U_p = 60$ eV.

ergy spectrum for circularly polarized light peaks at 64 eV, which is much higher than the 10 eV peak for linearly polarized light [22]. This general behavior is predicted by all the theories [5,12,18,19] and is due to the higher angular momentum possessed by the free electrons in ionization with circularly polarized light. Because the final electron states must conserve angular momentum, the low energy electron states are suppressed and the ionization threshold for circularly polarized light is about 1.5 times higher than for linearly polarized light. This has been observed for other atoms [3] and we have observed it in the ionization of Xe and He^{1+} in our laboratory. If the electric field is a circularly polarized monochromatic plane wave represented by $\mathbf{E}=(E_0/\sqrt{2})[\boldsymbol{\varepsilon}_x\cos(kx-\omega t)+\boldsymbol{\varepsilon}_y\sin(kx-\omega t)]$ then the total ponderomotive energy is still given by Eq. (2). The dashed line in Fig. 2 is a fit using the KFR model [18,19], where the transition probability rate per unit solid angle for n photon ionization is given by

$$\frac{dW_n}{d\Omega}=\frac{1}{(2\pi)^2\hbar^4}(2m_e^3)^{1/2}(n\hbar\omega-U_p)^2 \times(n\hbar\omega-U_p-I_p)^{1/2}|\Phi(p)|^2J_n^2(U_p^{1/2}\gamma)\,, \qquad (6)$$

where $\gamma=2(n\hbar\omega-U_p-I_p)^{1/2}/\hbar\omega$ and the J_n are the nth-order cylindrical Bessel functions. $\Phi(\mathbf{p})$ is the Fourier transform of the wave function shown in Eq. (5). Surprisingly the U_p that best fits the data is only 60 eV. In the quasistatic model the shape of the electron energy spectrum with circularly polarized light depends strongly on the temporal laser pulse shape. However, the peak of the electron energy distribution is always the same as the fit parameter U_p in that model, i.e., $U_p=64$ eV is the best fit parameter for the quasistatic model since the observed electron energy peak is 64 eV. Both these values of U_p are about 3.5 times less than the expected U_p (1.5×150 eV) from the fit to linear polarization data. The smaller peak intensities needed to fit the experimental data with circularly polarized light strongly contradict theoretical predictions.

In conclusion, we have measured short-pulse ATI electron spectra of He ionized at intensities up to 7×10^{15} W/cm^2 with both linearly and circularly polarized 820 nm light. These measurements test the models of ATI in the limit of ponderomotive energy $\gg$ ionization potential $\gg h\nu$. The ATI spectra do not agree well either with the KFR theory or with the dc tunneling theory followed by classical acceleration of the electron. Also, the fits to the data with linearly and circularly polarized light are not consistent with each other. The poor agreement between the theory and experiment can be due to Coulomb effect of the ions, which have been ignored in the models. Also the effect of doubly excited states and intermediate resonances, which play a more prominent role in linear polarization (more allowed angular momentum states), have to be included in the models. The results show that at these densities and this wavelength the electron temperature appears to be too hot to provide the fast recombination necessary for lasing in multiphoton-ionized recombination XUV lasers. The electron temperature might be lowered by using shorter wavelength lasers to multiphoton ionize the medium, since the ponderomotive energy (U_p) is proportional to λ^2; however, the failure of the models indicates that simple scaling arguments might not be appropriate.

*Present address: AT&T Bell Laboratories, Holmdel, NJ 07733.

[1] P. H. Bucksbaum, M. Bashkansky, and D. W. Schumacher, Phys. Rev. A **37**, 3615 (1988).
[2] R. R. Freeman, P. H. Bucksbaum, H. Milchberg, S. Darack, D. Schumacher, and M. E. Geusic, Phys. Rev. Lett. **59**, 1092 (1987).
[3] R. R. Freeman and P. H. Bucksbaum, J. Phys. B **24**, 325 (1991).
[4] J. H. Eberly, J. Javanainen, and K. Rzazewski, Phys. Rep. **204**, 331 (1991).
[5] P. B. Corkum, N. H. Burnett, and F. Brunel, Phys. Rev. Lett. **62**, 1259 (1989).
[6] B. Luther-Davies, B. W. Boreham, J. L. Hughes, and M. J. Hollis, J. Opt. Soc. Am. **68**, 658 (1978).
[7] S. Augst *et al.*, Phys. Rev. Lett. **63**, 2212 (1989).
[8] G. Gibson, T. S. Luk, and C. K. Rhodes, Phys. Rev. A **41**, 5049 (1990).
[9] M. D. Perry *et al.*, Phys. Rev. A **37**, 747 (1988).
[10] J. Peyraud and N. Peyraud, J. Appl. Phys. **43**, 2993 (1972).
[11] W. W. Jones and A. W. Ali, J. Appl. Phys. **48**, 3118 (1977).
[12] N. H. Burnett and P. B. Corkum, J. Opt. Soc. Am. B **6**, 1195 (1989).
[13] W. H. Knox and F. A. Beisser, *Ultrafast Phenomena VII*, edited by C. B. Harris, E. P. Ippen, G. A. Mourou, and A. H. Zewail (Springer-Verlag, Berlin, 1990).
[14] P. Maine, D. Strickland, P. Bado, M. Pessot, and G. Mourou, IEEE J. Quantum Electron. **24**, 398 (1988).
[15] J. F. Seeley and E. G. Harris, Phys. Rev. A **7**, 1064 (1973); W. L. Kruer, *The Physics of Laser Plasmas Interactions* (Addison-Wesley, New York, 1988), p. 3.
[16] L. V. Keldysh, Zh. Eksp. Teor. Fiz. **47**, 1945 (1964) [Sov. Phys. JETP **20**, 1307 (1965)].
[17] F. H. M. Faisal, J. Phys. B **6**, L89 (1973).
[18] H. R. Reiss, Phys. Rev. A **22**, 1786 (1980).
[19] H. R. Reiss, J. Phys. B **20**, L79 (1987).
[20] H. A. Bethe and E. S. Salpeter, *Quantum Mechanics of One- and Two-Electron Atoms* (Plenum/Rosetta, New York, 1977).
[21] P. M. Morse, *Thermal Physics* (Benjamin/Cummings, Reading, MA, 1969).
[22] The lower count rates in circular polarization are due to the larger emission solid angle (uniform distribution in the polarization plane). We have explicitly measured the angular dependence of emission for linear polarization. The electron distribution is peaked along the polarization axis with a full width half maximum of less than 15°–20° angular range.